HYPERSPECTRAL PAN-SHARPENING: A CONVEX FORMULATION TO IMPOSE PARALLEL LEVEL LINES

Alexis Huck, François de Vieilleville, Pierre Weiss and Manuel Grizonnet

A. Huck and F. de Vieilleville are with Magellium, Toulouse France
P. Weiss is with ITAV-USR3505, université de Toulouse, France
M. Grizonnet is with is with CNES, Toulouse, France.

ABSTRACT

In this paper, we address the issue of hyperspectral *pan-sharpening*, which consists in fusing a (low spatial resolution) hyperspectral image HX and a (high spatial resolution) panchromatic image P to obtain a high spatial resolution hyperspectral image. The problem is addressed under a convex variational constrained formulation. The fit-to-P data term favors high resolution hyperspectral images with level lines parallel to those of the panchromatic image. This term is balanced with a total variation term as regularizer. The fit-to-HX data is a constraint such that depends on the statistics of the data noise measurements. The developed Alternate Direction Method of Multipliers (ADMM) optimization scheme enables us to solve this problem efficiently despite the non differentiabilities and the huge number of unknowns.

Index Terms— hyperspectral, fusion, pan-sharpening, ADMM

1. INTRODUCTION

Hyperspectral sensors usually involve a trade-off between high spatial resolution and high spectral resolution. A common situation is that panchromatic images have a higher spatial resolution than hyperspectral images due to optics/photonics and cost considerations. Performing fusion between a (comparatively) low spatial resolution hyperspectral image and a (comparatively) high spatial resolution panchromatic image is a quite natural issue in order to estimate high spatial resolution hyperspectral data.

In the last three decades, pan sharpening approaches were dedicated to multispectral data. The earliest methods were based on specific *spectral-space transforms* such as the Hue-Intensity-Saturation (HIS) transform or the Principal Component Analysis (PCA) Transform. More recently, spatial frequency based approaches such as the High Pass Filter (HPF) method exploiting multiscale spatial analysis [1] provided improved results. The multiscale spatial analysis framework generally offers very time efficient performance but lacks flexibility to consider some prior knowledge about "physics of scene and sensor" (the sensors Modulation Transfer Function (MTF), sensor noise or any prior information). This aspect has been a limitation for application to hyperspectral pan sharpening. Thus, recent methods are generally based on variational [2] or bayesian [3] formulations. In particular, in [2], the authors have proposed to consider a term based on the topographic properties of the panchromatic image. This idea stems from [4] where the authors show that most geometrical information of an optical image lies in the set of its gray level-set lines.

The novelties of the proposed algorithm are threefold: 1. we propose a constrained convex formulation where the constraints are the fit-to-data terms. This enables to easily tune the related parameters which are the (supposed) known noise variances of the sensors. 2. The proposed minimization algorithm is based on the ADMM. It handles the non differentiabilities, constraints and special structures of the linear transforms in an efficient way. 3. The formulation takes the MTF (Modulation Transfer Function) into account, which helps refining the fit-to-hyperspectral-data constraint. This is favorable to high spectral fidelity in pan-sharpened hypersepctral data.

2. PROBLEM FORMULATION

In this paper, we rearrange (hyperspectral) images into vectors in order to allow writing matrix-vector products. Let $x = \begin{pmatrix} x_1 \\ \vdots \\ x_L \end{pmatrix} \in \mathbb{R}^{LM}$ and $u = \begin{pmatrix} u_1 \\ \vdots \\ u_L \end{pmatrix} \in \mathbb{R}^{LN}$ denote the low spatial resolution (LR) measured hyperspectral image and the (unknown) high spatial resolution hyperspectral image respectively. The integers L and M represent the number of spectral bands and the number of spectral pixels respectively. We let $p \in \mathbb{R}^N$ denote the rearranged panchromatic measured image, where $N = q^2 \times M$ and $q \geq 1$ denotes the resolution factor between the low and high resolution images. The linear projection operator which returns the l^{th} spectral band is

The authors would like to thank the CNES for initializing and funding the study and providing HypXim simulated data

denoted π_l. Then, $x_l = \pi_l x \in \mathbb{R}^M$ and $u_l = \pi_l u \in \mathbb{R}^N$ are the l^{th} spectral bands of x and u respectively.

A model formulation for any spectral band l of the hyperspectral measurements is given by

$$x_l = \mathrm{DH}u_l + n_{x_l}. \tag{1}$$

The linear operator $\mathrm{H} \in \mathbb{R}^{N\times N}$ respresents the spatial convolution with the spatial Point Spread Function of the hyperspectral sensor. The linear operator $\mathrm{D} \in \mathbb{R}^{M\times N}$ is a downsampling operator that preserves 1 every q pixels in the horizontal and vertical directions. Some additive sensor noise is considered in the vector n_{x_l}. We assume that $n_{x_l} \sim \mathcal{N}(0, \sigma^2_{x_l})$ where $\sigma^2_{x_l}$ is the noise variance of the l^{th} measured hyperspectral band.

A model formulation for the panchromatic image acquisition process is given by

$$p = \mathrm{G}u + n_p \tag{2}$$

where $\mathrm{G} \in \mathbb{R}^{N\times LN}$ is a linear operator which linearly and positively combines the spectral bands with weights equal to the samples of the spectral pattern of the panchromatic image. The noise of the measured panchromatic image is denoted $n_p \sim \mathcal{N}(0, \sigma^2_p)$.

Analogously to [2], we will exploit the fact that the different spectral bands of color images approximately share the same level lines. Such a knowledge can be integrated by comparing the gradient of the panchromatic data with the gradient of each hyperspectral image channel. A simple way to measure the discrepancy between the normal fields consist of using the function f below

$$f(u) = \sum_{l=1}^{L}\sum_{i=1}^{N} \left| \left\langle \nabla u_l(i), \frac{\nabla^\perp p(i)}{\|\nabla p(i)\|_2} \right\rangle_{\mathbb{R}^2} \right| \tag{3}$$

where $\nabla = \left[\partial_h^\intercal, \partial_v^\intercal\right]^\intercal : \mathbb{R}^N \to \mathbb{R}^N \times \mathbb{R}^N$ is the standard discrete gradient operator, ∂_h and ∂_v are the horizontal and vertical gradient operators respectively, $\langle\cdot,\cdot\rangle_{\mathbb{R}^2}$ is the standard Euclidian dot product in $\mathbb{R}^2$ and $\|\cdot\|_2$ the associated L_2 norm. The operator $\nabla^\perp = \left[-\partial_v^\intercal, \partial_h^\intercal\right]^\intercal : \mathbb{R}^N \to \mathbb{R}^N \times \mathbb{R}^N$ returns for each pixel a vector orthogonal to the gradient. Functional f has many attractive properties: it is convex in u and it can be shown to have a meaning in the continuous setting for bounded variation functions.

In natural scenes, the gradient can be very low in image areas corresponding to homogeneous radiometry of the scene. In such a case, f does not provide much information and an additional regularizing term should be added in the variational formulation. In this work, we use a standard total variation regularization [5], commonly used for such purposes and adapted in Eq. 4 to multiband images

$$TV(u) = \sum_{l=1}^{L}\sum_{i=1}^{N} \|(\nabla u_l)(i)\|_2 \tag{4}$$

where $\|\cdot\|_2$ is L_2-norm in $\mathbb{R}^2$. Note that we simply use total variation separately on each channel since the spectral information is accounted for using functional f. The proposed variational formulation for the hyperspectral pan-sharpening problem is as follows:

$$\begin{aligned} \hat{u} \;=\; & \underset{u}{\operatorname{argmin}}\ \gamma f(u) + (1-\gamma)TV(u) \\ s.t. \;\; & \|x_l - \mathrm{D}_s\mathrm{H}_s u_l\|_2^2 \le M\sigma^2_{x_l}, \forall l \in [1,\dots,L] \\ & \|p - \mathrm{G}u\|_2^2 \le N\sigma_p^2 \end{aligned} \tag{5}$$

where $\|\cdot\|_2$ denotes the L_2 norm in $\mathbb{R}^M$. In this formulation, $\gamma \in [0,1]$ fixes a balance between the two terms f and TV. The fit-to-data terms are constraints deriving from the physical models (Eq. 1 and 2). The parameters $(\sigma_{x_l})_{l\in\{1,\dots,L\}}$ and σ_p can be *a priori* given or estimated, which is a strong asset of the variational constrained formulation.

3. ADMM BASED OPTIMIZATION

Problem (5) is non differentiable, constrained and lives in very large dimensions. It can be solved using splitting techniques such as Arrow-Hurwicz or extragradient like methods [6] or ADMM based methods [7, 8]. There is recent theoretical and experimental evidence that ADMM like methods perform much better on some problem classes [9] and we thus decided to develop this method. Due to space limitations, we do not provide the details of the implementation. They follow closely the ideas suggested in [7, 8] and make use of: i) the simple structure of the linear transforms D_s and G, ii) the fact that H and ∇ can be diagonalized using the discrete Fourier transform and iii) the fact that the functions involved in equation 5 are l^1 or l^2-norms for which we can easily compute proximal operators. The proposed algorithm is called TVLCSP (for Total Variation iso-gray Level-set Curves Spectral Pattern).

4. EXPERIMENTAL RESULTS

We present here results of TVLCSP on AVIRIS [10] and simulated HypXim [11] data. We have first extracted a selection of the Cuprite scene (AVIRIS) which represents a mineral area. The $224-$spectral band data has been preprocessed and simulated as follows. 1 - Absorption spectral bands have been removed (bands: $1-6$, $106-114$, $152-170$ and $215-224$) to get a reference high resolution hyperspectral image u_{ref}. 2 - A convex combination of the spectral bands of u_{ref} gives the simulated panchromatic data p. The weights are the coefficients of the vector $\mathbf{g} = \left[\frac{1}{80}\dots\frac{1}{80}\right]$. 3 - The low resolution hyperspectral image x has been obtained from Eq. 1 without noise.

The chosen algorithm parameters are given in Table 1. Visual results are presented in Fig. 1.

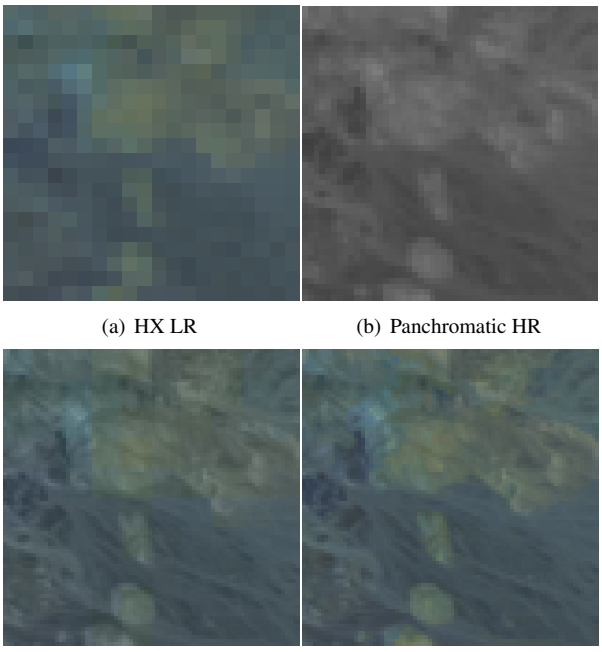

(a) HX LR (b) Panchromatic HR

(c) Wavelet HR estimation (d) TVLCSP HR estimation

Fig. 1. Cuprite scene and processing with wavelet and TVLCSP, for a resolution ratio $q = 4$

q	β	γ	σ_p	$\sigma_{\tilde{\mathbf{u}}}$	#iter
4	1000	0.01	0.0001	0.0001	300 & 3000

Table 1. Parameters of TVLCSP for the tests on the Cuprite scene.

In Table 2 we present quantitative evaluation and comparison with a wavelet-based pan-sharpening method [1] using usual performance metrics: 1 - global quality metrics RMSE and ERGAS, 2 - spectral quality metrics SAM and the spectral dispersion the spatial dispersion D_λ [12]), and 3 - spatial quality metrics FCC [13] and spatial dispersion D_s [12]. Note that D_λ and D_s are metrics without reference (ground truth high resolution hyperspectral image) requirement, which is relevant where no reference is available or when the reference is likely to introduce error in comparison (case of our HypXim data) due to noise.

Additionally, TVLCSP has been tested on simulated HypXim data. They have been simulated from data ac-

	TVLCSP		Wavelet
	#300	#3000	
RMSE ($\times 100$)	**0.48**	0.59	0.91
ERGAS	**5.45**	6.68	10.3
SAM	**0.61**	0.70	0.88
FCC ($\times 100$)	**99.3**	99.0	99.1
D_s ($\times 100$)	1.15	**0.89**	2.35
D_λ ($\times 100$)	1.82	**1.22**	4.43

Table 2. Performances of pan-sharpening algorithms on the Cuprite subimage.

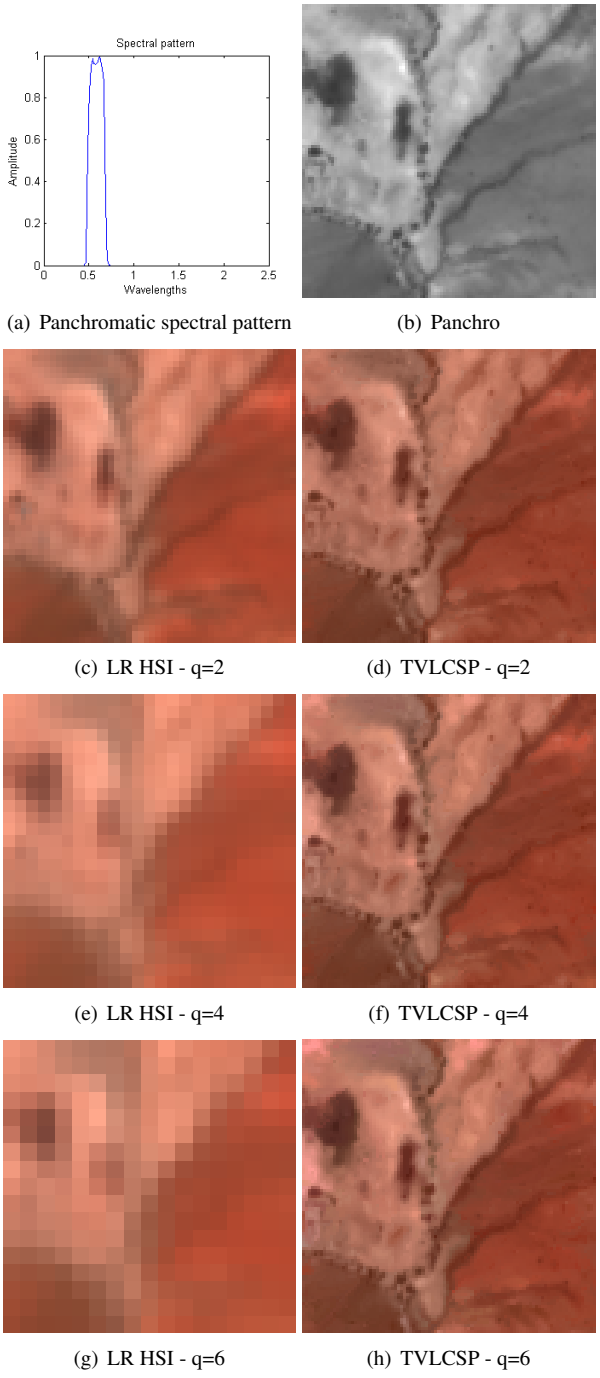

(a) Panchromatic spectral pattern (b) Panchro

(c) LR HSI - q=2 (d) TVLCSP - q=2

(e) LR HSI - q=4 (f) TVLCSP - q=4

(g) LR HSI - q=6 (h) TVLCSP - q=6

Fig. 2. HypXim scene and processing with TVLCSP, for resolution ratios $q = 2$ and $q = 6$.

q	Spatial resolution (m)	Sumulated sensor
1	4.80	Panchromatic sensor
1	4.80	Reference
2	9.60	HypXim P (Performance concept)
4	19.20	HypXim C (Challenging concept)
6	28.80	ENMAP

Table 3. Characteristics of the simulated HypXim and panchromatic data.

	$q=2$	$q=4$	$q=6$
RMSE $\times 100$	1.73	2.08	2.29
ERGAS	11.5	28.5	47.0
SAM	1.57	1.50	1.64
FCC $\times 100$	97.6	97.3	97.2
D_s $\times 100$	3.05	4.28	4.59
D_λ $\times 100$	3.41	2.30	1.82

Table 4. Performances of TVLCSP on the HypXim sub-image

.

quired in the framework of the Pléiades program. The scene is located in Namibia and a sub-scene has been extracted. The characteristics of the considered data are given in Table 3. The considered sensitivity spectral pattern is shown in Fig. 2(a). We see that only some (20) of the spectral bands contribute to the panchromatic data thus only 20 non-zero coefficients in $\mathbf{g}$ and the presented result only concerns these bands. Note that the hyperspectral sensor spatial Point Spread Functions (PSF) has been supposed Gaussian spectrally and spatially invariant, with a parameter tuned experimentally. The visual results are presented in Fig. 2 and the corresponding performance metrics are given in 4. Results on HypXim are not as good as those on AVIRIS, probably due to our approximation hypotheses on the sensor parameters and to the presence of noise. Note that the simulated reference image is corrupted by sensor noise whereas TVLCSP provides relatively denoised data estimations, which introduces lack of confidence in the performance metrics values.

5. CONCLUSION

We have tackled the pan-sharpening problem using a constrained viariationnal approach with an objective based on the conservation of iso-gray level set lines among spectral bands and total variation. The fit-to-data constraints have been mathematically considered as such and are based on the signal model and the sensor parameters, including noise statistics. An ADMM scheme has been developped, called TVLCSP and evaluated on AVIRIS and HypXim simulated data.

6. REFERENCES

[1] T. Ranchin and L. Wald, "Fusion of high spatial and spectral resolution images: the arsis concept and its implementation," *PERRS*, vol. 66, no. 1, pp. 49–61, 2000.

[2] C. Ballester, V. Caselles, , L. Igual, and J. Verdera, "A variational model for p+xs image fusion," *IJCV*, vol. 69, no. 1, pp. 4358, 2006.

[3] M. Joshi and A. Jalobeanu, "MAP estimation for multiresolution fusion in remotely sensed images using an IGMRF prior model," *IEEE TGRS*, vol. 48, no. 3, pp. 1245–1255, 2010.

[4] V. Caselles, B. Coll, and J.-M. Morel, "Geometry and color in natural images," *JMIV*, vol. 16, no. 2, pp. 89–105, 2002.

[5] L.I. Rudin, S. Osher, and E. Fatemi, "Nonlinear total variation based noise removal algorithms," *Physica D*, vol. 60, no. 1-4, pp. 259–268, 1992.

[6] A. Chambolle and T. Pock, "A first-order primal-dual algorithm for convex problems with applications to imaging," *JMIV*, vol. 40, no. 1, pp. 120–145, 2011.

[7] S. Boyd, N. Parikh, E. Chu, B. Peleato, and J. Eckstein, "Distributed optimization and statistical learning via the alternating direction method of multipliers," *Found. and Trends in Mach. Learn.*, vol. 3, no. 1, pp. 1–122, 2011.

[8] M. Ng, P. Weiss, and X. Yuan, "Solving constrained total-variation image restoration and reconstruction problems via alternating direction methods," *SIAM SC*, vol. 32, no. 5, pp. 2710–2736, 2010.

[9] Daniel Boley, "Local linear convergence of the alternating direction method of multipliers on quadratic or linear programs," *SIAM Opt*, vol. 23, no. 4, pp. 2183–2207, 2013.

[10] "Aviris," http://aviris.jpl.nasa.gov/.

[11] R. Marion, V. Carrere, S. Jacquemoud, S. Chevrel, P. Prastault, M. D'oria, P. Gilouppe, S. Hosford, B. Lubac, and A. Bourguignon, "Hypxim: A new hyperspectral sensor combining science/defence applications," in *WHISPERS*, 2011.

[12] Luciano Alparone, Bruno Aiazzi, Stefano Baronti, Andrea Garzelli, Filippo Nencini, and Massimo Selva, "Multispectral and panchromatic data fusion assessment without reference," *PERRS*, vol. 74, no. 2, pp. 193–200, 2008.

[13] Z. Zhou, D.L. Civico, and J.A. Silander, "A wavelet transform method to merge landsat TM and SPOT panchromatic data," *IJRS*, vol. 19, no. 4, 1998.